Heat Mass Transfer (2017) 53:1603–1617
DOI 10.1007/s00231-016-1926-y

ORIGINAL

Assessment of suitability of some chosen functions for describing of sorption isotherms in building materials

Agata Stolarska[1] · **Halina Garbalińska**[1]

Received: 6 April 2016 / Accepted: 4 October 2016 / Published online: 12 October 2016

Abstract This paper presents results of tests and studies conducted on six common building materials, used for constructing and finishing of external walls. These included: ceramic brick, silicate brick, autoclaved aerated concrete, cement mortar, cement–lime mortar and cement mortar modified with polypropylene fibers. Each of these materials is distinguished by the other structure of porousness, affecting both the course of sorption processes and the isotherms obtained. At first, measurements of moisture sorption kinetics at temperatures of 5, 20 and 35 °C were performed, each time at six levels of relative humidity. Then, when the sorption processes expired, equilibrium moisture sorption values were determined for the materials in 18 individual temperature and humidity conditions. The experimental data were used to determine the sorption isotherm courses for each material at the three temperatures. Then, theoretical analysis was performed in order to determine, which of the models available in the literature described the sorption isotherms of the concerned building materials the best. For each material and each of the three temperature values, twenty-four equations were tested. In each case, those of them were identified which ensured the best matching between the theoretical courses and the experimental data. The obtained results indicate that the Chen's model proved to be the most versatile. It ensured a detailed description of the sorption isotherms for each material and temperature tested.

✉ Agata Stolarska
siwinska@zut.edu.pl

Halina Garbalińska
Halina.Garbalinska@zut.edu.pl

[1] Faculty of Civil Engineering and Architecture, West Pomeranian University of Technology Szczecin, Aleja Piastów 50, 70-311 Szczecin, Poland

List of symbols

A, B	Coefficients determined experimentally for a given system and temperature
AAC	Autoclaved aerated concrete
CB	Ceramic brick
CLM	Cement–lime mortar
CM	Cement mortar
C, D	Constant
E	Characteristic energy of adsorption
K_1, K_2, K_n	Constants
K	Henry's constant
MM	Modified mortar
SB	Silicate brick
R	Correlation coefficient
R	Gas constant (J/mol K)
T	Temperature (°C)
W_0	Micropore volume
a	The amount of adsorbed substance (kg/kg)
a_m, a_0	Monolayer capacity (kg/kg)
a_s	Constant
a″, b″	Constants of Jovanovič's function for multilayer adsorption
a, b, c	Experimentally determined values
d	Parameter $d = 1/(u_{hig}B)$
$h = p/p_s$	Relative vapour pressure (%)
k, k_1, k_2, n, s	Constant
m	Water content in samples (%)
m_d	Dry sample mass (g)
m_e	Mass in the state of moisture equilibrium (g)
p	Vapour pressure (Pa)
p_s	Saturated vapour pressure (Pa)

t	Toth's parameter
t	Time (h)
u_L	Weight moisture content
u_{hig}	Saturation hygroscopic, determined experimentally
w	Sorption dampness (%)

Greek symbols

α, α_m	Constants
φ	Air relative humidity (%)
ρ_c	The density of the adsorbate (g/cm^3)
υ	The volume of vapour adsorbed
Θ	The level of the mono-layer coverage of the adsorbent surface

1 Introduction

Dampness of building materials is a factor recognized as critical. This can be attributed to the destructive impact of moisture to durability of building materials (e.g. Jenisch [1], Rahn and Bonk [2]) and such their technical parameters, as: strength (e.g. Unčik et al. [3]), frost-resistance (e.g. Garbalińska and Wygocka [4], Wygocka [5]), thermal conductivity (e.g. Siwińska [6], Siwińska and Garbalińska [7]) and others. In order to define the quantitative relationships between the balance moisture contained in the material and the moisture-related conditions existing in the ambient air, sorption isotherms are determined, the course of which depends not only on the material porous structure, but on the temperature as well.

For many years, in many scientific centers, research works have been conducted on moisture sorption processes in building materials. In general, the sorption research consists of determining the adsorbate mass, based on precise measurements of the sample mass before and after the experiment, i.e. after the mass got stabilized. The way of determining the sorption characteristics with the standard method is described in the norm PN-EN ISO 12571:2002 [8]. Its drawbacks and application of a new method (APM Augenblicksprofilmethode, IPM Instantaneous Profile Method), which shortens the time, were presented by Plagge et al. [9–11], Scheffler et al. [12]. On the other hand, Markova et al. [13], Wadsö and Wadsö [14] presented a novelty measuring method, using the so called microcalorimeter, which permits thermodynamic description of the process of sorption. A dynamic vapour sorption (DVS) system was used to determine sorption isotherms in McGregor et al. [15, 16] and Wu et al. [17].

Sorption of the mortars, which inter alia were the subject of this paper, was studied also by Anderberg and Wadsö [18], Espinosa and Franke [19], Janz [20], Johannesson [21]. Another team of Garbalińska et al. [22] focused on cement mortars with a different w/c ratio, tested at five relative humidity ranges and in the desorption process. A dynamic determination of sorption isotherm also of cement based materials was performed in Tada and Watanabe [23]. A frequent object of tests and studies was autoclaved aerated concrete, tested, for instance, in Jerman et al. [24]. Those studies of sorption were conducted on autoclaved aerated concrete with different bulk density. However in Koronthalyova [25], there were presented results of the research concerning moisture storage capacity and microstructure of ceramic brick and autoclaved aerated concrete. The tests referred to materials coming from different manufacturers. On the other hand, Jiřičková and Černý [26] presented test results for moisture parameters of materials based on mineral wool. For the tested materials, they determined a sorption isotherm at 20 °C, at eight levels of sorption dampness. An assessment of moisture qualities of hemp as insulation material was performed in Valovirta and Vinha [27]. In their studies, Valovirta and Vinha focused on hemp in the loose form and three types of insulation in the form of mats. For those materials, sorption isotherms were drawn at five levels of sorption dampness. Moisture-related qualities of many popular building and insulating materials (37 materials) were also assessed by Kumaran [28] in his work. Among many experimentally determined parameters, Kumaran determined sorption isotherms, as well. In the case of sorption measurements, the samples were sized 40 × 40 × 20 mm (8 pieces for a measurement at φ = 100 %, T = 22 °C) and 40 × 40 × 6 mm (3 pieces for measurement at φ = 88.1; 71.5; 0.6 %, T = 23 °C). An assessment of the impact of adding some glass fibers to cement mortar to its moisture-wise parameters was presented in Poděbradská et al. [29]. Team of Poděbradská tested three mortars, different with their composition, content of the fibers and applied additives.

The tests, which were described in the literature, performed in various centers, are the sign of a wide range of problems discussed in relation to sorption of moisture in building materials. To high extent they concern the influence of different factors on the scale of the equilibrium dampness. They also give evidence of a diversification of research techniques applied.

The experimentally determined equilibrium sorption moisture values are used for determining sorption isotherms, which are then attempted to describe in mathematical categories. One has to note that the literature provides a lot of empirical equations of adsorption isotherms, developed for particular purposes and using various concepts and also some new mathematical techniques, as, for instance, neuron networks or genetic codes (Keller and Staudt [30]). Nevertheless, there is no universal sorption isotherm equation available, which could describe satisfactorily the course of this curve for all building materials, in the entire

relative humidity. Thus, the analysis get down to verification of equations available in the ever-growing literature of the subject (Chen and Chen [31], Kumar [32], Kumar and Sivanesan [33, 34], Keller and Staudt [30], Lowell et al. [35], Lagorosse et al. [36], Osanyintola and Simonson [37], Perry and Green [38], Rouquerol et al. [39], Yuh-Shan [40], Pavlik et al. [41], Furmaniak [42]), while the authors achieve various degrees of adjustment of their theoretical curves to the courses observed in the experiments.

In the extensive literature of physical chemistry, two classifications of sorption isotherms dominate, namely the Brunauer's classification (Perry and Green [38], Rouquerol et al. [39], Brunauer et al. [43]) and the one of IUPAC (Keller and Staudt [30]; Rouquerol et al. [39], Lowell et al. [35]). Materials of different internal structures present different kinetics of the adsorption process and different balance dependencies. Therefore it is difficult to find one ideal function, which could describe sorption isotherms for all materials in a satisfactory manner. A number of frequently used empiric description of adsorption isotherms, referring to non-organic, organic and biological materials of the adsorbent, can be found in Keller and Staudt [30], where references to sources providing a broad review of isotherms are given.

In this paper, suitability of 24 mathematical models, describing dependence of sorption dampness on relative humidity, are analyzed and assessed. In many cases in study, equations were insufficient to give a full explanation or description of processes taking place during the sorption process. Namely, we come across Henry's dependence at very low pressures. With this equation, at a very low pressure of the gas, adsorption value is proportional to concentration or pressure in the volumetric phase. On the other hand, in Langmuir's equation, within the scope of low pressers in the gaseous phase, adsorption is proportional to steam pressure and in this range of pressures Langmuir's equation gets transformed into Henry's equation [30]. As far as Langmuir's isotherm is concerned, the value of adsorption grows initially proportionally to pressure, and after some time this growth ceases gradually, and at sufficiently high pressures of the gas adsorption achieves a constant value. At that time, the adsorbent surface becomes saturated with a one-molecule layer of adsorbate. Langmuir's isotherm describes chemi-sorption cases quite well. In case of physical adsorption, it reflects the reality well only for small degrees of coverage, failing at higher pressure values. The course of Langmuir's isotherm features a linear section within the scope of low pressures and a proximity to a horizontal line for higher pressures. On its whole length the isotherm is convex. The isotherm is usable the most for describing adsorption in micro-porous materials [30]. Langmuir's isotherm equation is frequently an initial equation for a number of more detailed studies, as in many cases it is not sufficient for getting a full picture of what is really happening. On the other hand, Freundlich's equation does not always deliver a satisfactory set of values calculated with those experimental ones, especially for higher pressures. According to this equation, quantity of the adsorbed substance may increase with no limits, along with the growth of the pressure, while, in fact, the phenomenon of saturation occurs. The Freundlich's isotherm equation describes adsorption on heterogenic surfaces and experimental data for small concentrations pretty well. Meanwhile, erroneous results may be achieved with Dubinin and Raduszkiewicz's equation—particularly, where a microporous adsorbent is heterogenic [35].

Another theory, the BET theory, hardly ever describes the isotherms for the entire relative pressure range [35]. The BET model fails for adsorbents with a porous structure because of capillary condensation. The BET isotherm is correct within the p/p_s range (relative partial steam pressure) up to 0.5. For pressures close to saturated steam pressure values the compliance is worse, where for $p/p_s = 1$ the dependence of the adsorbed gas amount on p/p_s departs from the one described with the BET equation. The BET equation envisages a too low adsorption under a low pressure and a too high adsorption under a high pressure. According to [30, 35], the BET equation can be used for $0.05 < p/p_s < 0.35$, and sometimes 0.5. For $p/p_s > 0{,}5$ the BET equation loses its suitability because of the occurrence of physical adsorption and capillary condensation. It is not recommended to use the BET equation for adsorbents with very narrow pores. The Harkins–Jury's equation ensures a larger range of coherence with experiments than the BET equation does. One of modifications of the BET equation is the Hüttig's adsorption isotherm. Another formula, the Hansen's equation, describes the course of sorption isotherms within the humidity range from 20 to 98 %. According to information available in the literature, for conditions with low pressure and high temperature values, physical adsorption of gas molecules decreases and the isotherms are a straight-line function as the Henry's or Freundlich's ones. For high pressures and low temperatures physical adsorption of gas molecules grows and we may expect isotherms similar to those of the Langmuir's. On the other hand, at high pressures and low temperatures physical adsorption leads to condensation in the pores and isotherms typical of the BET can be expected.

Many models of sorption isotherms, including the ones mentioned above, were tested on building materials.

A popular cellular concrete, was subject to studies presented in [44]. Its authors tested that material for seven temperature values (5, 10, 15, 20, 25, 30, 35 °C) on small (30 × 30 × 10 cm) and large (40 × 40 × 20 cm) samples. For getting a description of the sorption isotherms obtained from the nine tested models, the Oswin equation

Table 1 The parameters of the materials tested

Material	Density (g/cm^3)	Specific surface (m^2/g)	Tortuosity of pores (−)	Porosity (%)
CB	1.547	2.419	1.879	41.313
SB	1.727	7.723	2.019	25.306
AAC	0.626	41.413	1.682	67.090
CM	2.053	6.445	2.137	12.901
MM	2.004	7.433	2.126	14.884
CLM	1.681	7.097	2.040	26.642

proved to be the best. The same material was studied by the authors of [45], as well, but this time for one temperature of 25 °C and eight humidity levels. Seven models were analyzed. Again, two sample sizes were tested (small ones: 3 × 3 × 1× cm and large ones: 4 × 4 × 2× cm). As a result of analyzing many equations, the authors chose their own new model as the best.

According to the data available in the literature, in case of many building materials, the above mentioned equations do not reflect the form of the isotherms with a sufficient precision for the entire scope of relative humidities. Hence, referring to the whole range of pressures, from $p/p_s = 0$ to $p/p_s = 1$, we may say that for such a type of materials it is impossible to identify a simple isotherm, which would make it possible to describe all the phenomena of physical adsorption, taking place where gas is in touch with the surface of porous solid bodies. This is the effect of the energetic heterogeneity on the adsorption surfaces, an intense diversification of the shapes of the pores, their sizes, mutual interconnections and various qualities of adsorbed molecules. Nevertheless, the above mentioned isotherm equations find their practical application in experiments or industrial processes [30]. When describing experimental data, many scientists use those models, as e.g. [36, 40], and obtain high coherence. Some reach for linearized forms of the equations to estimate the isotherm parameters, e.g. Kumar and Sivanesan [32–34].

Having that in mind, the authors found it recommendable to make an attempt to describe sorption isotherms for some selected popular building materials, using the approximating functions that are proposed in the literature. The authors focused, however, only on those, for which their suitability in engineering has been proven. Bearing in mind studies presented in the literature, the authors decided to conduct an extensive experiment on moisture sorption and to analyse a mathematical description of the obtained experimental data. In this paper, suitability of 24 mathematical models describing dependence of sorption dampness on relative humidity, were analyzed and assessed. As the tested materials were used: ceramic brick, silicate brick, autoclaved aerated concrete and three different cement-based mortars. The results and the obtained dependencies of the dampness on the relative humidity w(φ), determined for each of the materials concerned at three temperature levels, are presented below.

2 Experimental

2.1 Tested materials

Six commonly used building materials, used for erection and finishing of external walls, were tested. The performed measurements concerned three types of brick and three mortars based on cement, with the following contents in 1 dm^3:

- cement mortar CM: cement 490, water 270, sand 1519 g,
- modified mortar MM: cement 490, water 270, sand 1519 g, polypropylene fibers with length of 3 mm 0.9 g,
- cement–lime mortar CLM: cement 194, lime 194, water 336, sand 1164 g.

In the brick group, the common, full ceramic brick CB, autoclaved aerated concrete AAC and silicate brick SB were tested. The data on the materials tested are collected in Table 1. Their specific gravity and structural parameters were determined by means of the Pore Master 60 mercury porosimeter. The parameters given in Table 1 were determined considering specific capacity of the measuring instrument available. Mercury porosimeter, used in the measurements, enables to assess data for the pores of diameters from ≈950 to ≈0.003 μm. The method applied is the most common technique used to measure structural parameters of porous building materials, also those which were the subject of the research performed. The textural parameters obtained by Mercury Intrusion Porosimetry will be supplemented in the future by additional data from measurements performed with the application of scanning electron microscopy. The SEM analysis it will make it possible to perform both an assessment of the chemical composition using energy dispersive spectroscopy analyzer, but also to identify better the microstructural details of the tested materials. It will enable a more complete analysis

Table 2 The values of the relative humidity above saturated solutions in the state of equilibrium

5 °C		20 °C		35 °C	
Salt	φ (%)	Salt	φ (%)	Salt	φ (%)
LiCl	11.26 ± 0.47	LiCl	11.31 ± 0.31	LiCl	11.25 ± 0.22
$MgCl_2$	33.60 ± 0.28	$MgCl_2$	33.07 ± 0.18	$MgCl_2$	32.05 ± 0.13
$Mg(NO_3)_2$	58.86 ± 0.43	$Mg(NO_3)_2$	54.38 ± 0.23	$Mg(NO_3)_2$	49.91 ± 0.29
NaCl	75.65 ± 0.27	NaCl	75.47 ± 0.14	NaCl	74.87 ± 0.12
KCl	87.67 ± 0.45	KCl	85.11 ± 0.29	KCl	82.95 ± 0.25
K_2SO_4	98.48 ± 0.91	K_2SO_4	97.59 ± 0.53	K_2SO_4	96.71 ± 0.38

of the influence of microstructural parameters on moisture sorption processes.

2.2 Moisture sorption measurements

In order to propose a function dependence, which could provide a satisfactory description of the relationship between the material moisture content w and the air relative humidity φ, it was necessary to conduct tests aimed at determining the values equilibrium sorption dampness at different ambient conditions.

The moisture sorption studies were performed according to norm PN-EN ISO 12571:2002 [8]. They were conducted at three temperatures and at six relative humidity levels:

$$\mathrm{T} = 5\,^{\circ}\mathrm{C} : \varphi \approx 11,\ 34,\ 59,\ 76,\ 88,\ 98\,\%,$$
$$\mathrm{T} = 20\,^{\circ}\mathrm{C} : \varphi \approx 11,\ 33,\ 54,\ 75,\ 85,\ 98\,\%,$$
$$\mathrm{T} = 35^{\circ}\mathrm{C} : \varphi \approx 11,\ 32,\ 50,\ 75,\ 83,\ 97\,\%.$$

Maintenance of the temperature at the desired level was ensured by means of a chamber thermostat, while stability of the relative humidity was obtained by means of saturated water solutions of appropriate salts: LiCl, $MgCl_2$, $Mg(NO_3)_2$, NaCl, KCl, K_2SO_4. Use of the mentioned saturated salt solutions in the Raoult's law. The saturated conditions were ensured by the presence of crystals of salt at the bottom of the vessel, whereas only the molecules of the solvent, i.e. water reached the space above the solution and provided the appropriate air relative humidity. Table 2 shows the values of the air relative humidities above the saturated solutions in the state of equilibrium at three temperature levels pursuant to PN-EN ISO 12571:2002 [8] standard including the uncertainty interval for the each temperature. The samples of the materials tested were situated on a grille above the saturated solutions and there was no contact between them.

The selected materials were cut into 1 cm thick samples, insulated on the side surfaces and dried up to constant mass in a dried adjusted to the temperature of 105 °C. Next, the samples were put in tight containers with the particular solutions and the containers were moved into a climatic chamber with a stable temperature. In the thermostatic chamber, in each air-tight container, three samples of each material were stored.

The sorption measurements came down to recording the changes the mass of the samples. At the commencement of the research (t = 0 h), the samples were completely dried. The process of absorption of humidity in each climate (at $\varphi > 0$ %) manifested by the mass increase. The intervals among each particular weighing, initially being of 6, 8, 12 h, extended gradually to 7 days. The measurements were performed until the moisture equilibrium was achieved in all the samples kept in the given thermal/humidity conditions. The tests were continued for 6 months (temperatures 5 and 20 °C) and 5 months (35 °C) for the wall materials, and for 9 months (20 and 35 °C) and 10 months (5 °C) for the mortars.

The graphs, showing the kinetics of the sorption process at the temperature of 20 °C for three mortars (CM, MM, CLM) can be found in the article [7]. Below are shown the graphs (Figs. 1, 2, 3) for the remaining materials (CB, SB, AAC) obtained at the temperature of 20 °C for six levels of humidity φ. The entire set of the graphs for all the temperatures and materials is included in the study [6].

Most intensively, the sorption process took its course in the initial phase, i.e. during the first 7 days. Afterwards only some slight increments in the sorption dampness were observed, extended, however over many months. Obtained for the equilibrium state, the results were used for determining the sorption dampness w (%), expressed as a percentage of water content, referred to the dry sample mass:

$$w = \frac{m_e - m_d}{m_d} \times 100 \tag{1}$$

For each of the 18 climatic conditions, the stabilized sorption dampness w was determined as an arithmetic mean of the three samples. The test results were shown in Tables 3, 4, and 5.

Among all the materials in study, the highest sorption dampness was recorded for autoclaved aerated concrete at 5 °C and $\varphi \approx 98$ %, amounting to 25.25 %. The lowest equilibrium dampness in each of the climates in question was observed in the ceramic brick—it featured a very low sorptivity, not exceeding 2 %.

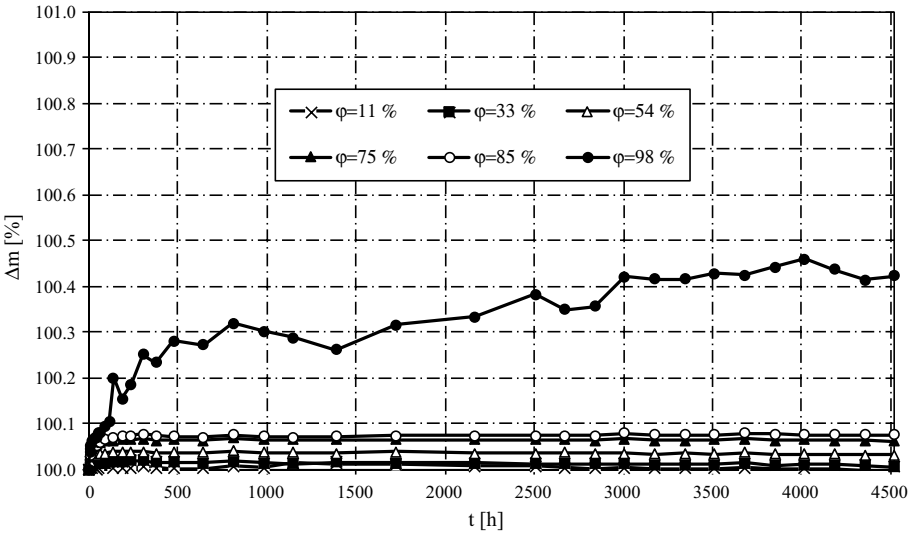

Fig. 1 Kinetics of sorption process for ceramic brick (CB), T = 20 °C

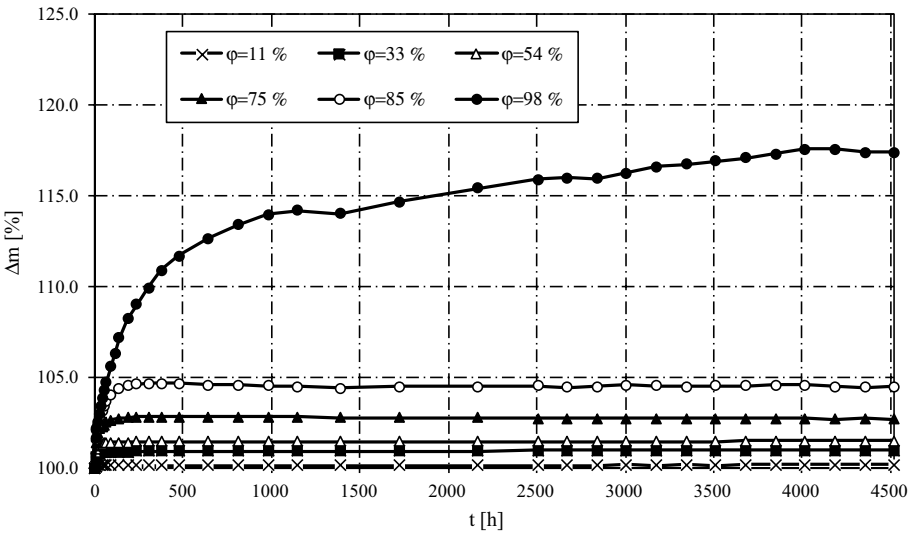

Fig. 2 Kinetics of sorption process for silica brick (SB), T = 20 °C

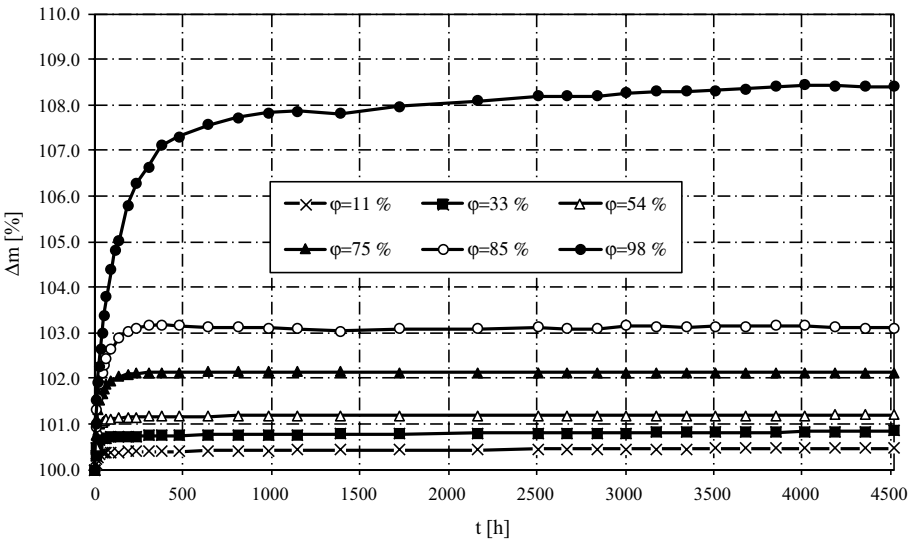

Fig. 3 Kinetics of sorption process for autoclaved aerated concrete (AAC), T = 20 °C

Table 3 Mean stabilized sorption dampness w at 5 °C for all materials

φ (%)	CB w [%]	SB w [%]	AAC w [%]	CM w [%]	MM w [%]	CLM w [%]
11	1.789	1.885	4.163	0.878	0.831	0.561
	1.457	2.078	4.162	0.922	1.332	0.622
	1.286	2.077	4.063	1.017	0.801	0.590
Average	1.51	2.01	4.13	0.94	0.99	0.59
34	1.274	2.271	3.670	1.563	1.614	0.944
	1.282	2.354	5.212	1.578	1.439	0.956
	1.194	2.489	4.656	1.392	1.332	1.010
Average	1.25	2.37	4.51	1.51	1.46	0.97
59	1.125	2.945	5.268	2.375	2.122	1.674
	1.176	2.917	4.561	2.438	2.667	2.154
	0.965	3.019	5.028	2.450	2.106	1.687
Average	1.09	2.96	4.95	2.42	2.30	1.84
76	1.418	3.639	5.840	3.849	3.239	2.989
	1.228	3.821	6.321	3.511	3.153	3.250
	1.071	3.834	5.494	3.241	3.508	5.030
Average	1.24	3.76	5.89	3.53	3.30	3.76
88	1.557	6.332	10.329	5.997	6.638	5.097
	0.946	6.387	9.231	5.567	6.667	4.989
	0.998	6.105	9.788	5.828	6.281	5.653
Average	1.17	6.28	9.78	5.80	6.53	5.25
98	1.816	10.015	26.216	9.581	8.087	10.329
	1.888	10.032	25.203	8.539	8.606	11.339
	1.923	10.162	24.318	7.363	8.549	14.202
Average	1.88	10.07	25.25	8.49	8.41	11.96

2.3 Sorption isotherms: experimental results

Experimental data permitted to draw up sorption isotherms for the tested materials at the each of tested temperatures. Figure 4 gathers the sorption isotherms, drawn for each of the six materials at the three temperatures.

The presented above groupings of obtained curves confirmed the influence of both the various structures of the tested materials, and the temperature on the nature of sorption isotherms. An assessment of the impact of temperature on the character of sorption isotherms was based on the graphs shown on Fig. 4. For the ceramic brick, no noticeable influence of temperature on the obtained isotherms was observed in the entire humidity range. For the other materials, the influence of the temperature on the course of the isotherms of sorption was manifested in a clearer way particularly in the scope of the higher humidities $\varphi > 75$ %. There, a specific tendency is clearly seen, as the curves determined for 5 °C remain above the other ones. At 35 °C the isotherms generally are distinguished with the lower values of the equilibrium humidities.

In the case of structural materials (CB, SB, AAC) it was observed that the isotherms do not match one another throughout the entire range of the tested humidity, at each of the temperature levels chosen for the tests. The isotherms indicate plainly different internal structures of those materials. The cellular concrete, i.e. the material of the highest porousness and the specific surface, demonstrated the highest values of the sorption humidity in particular climates.

As far as the mortar group is concerned, the situation is quite different. The isotherms of the cement and modified mortars (CM, MM) are very similar at the three temperature values. Generally, the polypropylene fibers that had been added to the modified mortar did not affect the course of the sorption isotherm, while addition of lime to the mortar (CLM) contributed to the fact that the cement–lime mortar isotherm locates itself below the curves determined for the other two mortars.

The achieved sorption isotherms run smoothly from the moment of formation of a single adsorption film, through appearance of other layers, until the beginning of capillary condensation, when the dampness grows dramatically. The observable differences concerning the sorption dampness value in the materials in question and the course of the sorption isotherms are attributed to different specific surface areas of the tested materials and their different porosity structures. Only when relative moisture grew above 90 %, at all the temperature values, i.e. 5, 20 and 35 °C, the

Table 4 Mean stabilized sorption dampness w at 20 °C for all materials

φ (%)	CB w [%]	SB w [%]	AAC w [%]	CM w [%]	MM w [%]	CLM w [%]
11	1.098	1.602	3.744	0.755	1.029	0.410
	1.292	1.606	3.922	0.739	0.976	0.541
	1.260	1.837	3.572	0.718	1.002	0.560
Average	1.22	1.68	3.75	0.74	1.00	0.50
33	0.733	2.235	4.959	1.259	1.762	1.212
	1.211	2.163	4.382	1.307	1.692	0.949
	1.475	2.077	5.329	1.810	1.705	1.007
Average	1.14	2.16	4.89	1.46	1.72	1.06
54	1.408	2.507	5.325	2.320	2.246	1.377
	1.353	2.473	4.528	2.519	2.138	1.373
	1.304	2.421	5.319	2.506	2.381	1.382
Average	1.36	2.47	5.06	2.45	2.26	1.38
75	1.036	3.203	6.125	4.142	3.917	2.892
	1.139	3.455	6.212	3.909	3.810	2.899
	1.162	3.308	6.047	3.766	3.418	3.435
Average	1.11	3.32	6.13	3.94	3.72	3.08
85	1.157	4.488	7.718	5.017	4.890	4.077
	1.091	3.785	7.982	5.708	4.924	3.701
	1.312	4.620	7.964	4.234	4.808	3.578
Average	1.19	4.30	7.89	4.99	4.87	3.79
98	1.616	9.663	21.273	7.104	7.913	8.375
	1.513	12.346	21.504	7.238	8.041	8.038
	1.840	9.435	22.052	8.042	8.351	8.041
Average	1.66	10.48	21.61	7.46	8.10	8.15

isotherms of the ceramic brick disclosed a slight increase in the material dampness. For silicate brick and autoclaved aerated concrete, the obtained isotherms disclose three stages of adsorption clearly. Their first sections are convex. Their points of inflexion and increase of moisture above 80 % are clearly shown.

For cement-based materials, the courses of isotherms are more moderate. Similarly to the other materials, sorption isotherms of mortars can be qualified as type II in the Brunauer's and IUPAC classifications.

2.4 Estimation of sorption isotherms

The main objective of this study was to test the possibility of describing the experimentally obtained isotherms, applying the sorption isotherm equations proposed in the literature. Several dozens of equations, drawn from the extensive literature of the subject, were used. The authors decided to perform such a big testing scheme in terms of the equations suitability because of the fact that the literature they referred to did not offer any universal model that could help describe experimental data in a satisfactory way in reference to different materials, within the entire relative humidity range and at different temperature levels. Functions used in the analysis are presented in Table 6 (Chen and Chen [31], Keller and Staudt [30], Siwińska [6]).

With statistical methods, compliance of the adsorption isotherm equations (Table 6), as proposed in the literature, with experimental data was determined. For that purpose the STATISTICA programme was used. To estimate the coefficients of the equations, the authors used one of the programme modules, i.e. the non-linear estimation. To assess the quality of the coherence between the equations to the experimental data, correlation coefficient R and the least squares estimator were used (Yuh-Shan [40]). Two estimation methods, the ones of Levenberg–Marquardt's and Gauss–Newton's were applied. The data collected in Table 7 manifest to what extent the models tested are suitable to description of the isotherms of sorption for each of the materials in a given temperature. Lack of specified value of the R parameter manifests lack of such possibility.

The values of the R parameters placed in Table 7 show the accuracy of matching provided by a given model.

In Figs. 5, 6, 7, 8, 9 and 10 the authors presented graphs for each of the materials at the three temperature levels, obtained with the application of the best experiment-matching equations, i.e. the ones, for which the values of R were the highest (shown bold in the Table 7).

Table 5 Mean stabilized sorption dampness w at 35 °C for all materials

φ (%)	CB w [%]	SB w [%]	AAC w [%]	CM w [%]	MM w [%]	CLM w [%]
11	1.233	1.546	3.309	0.838	1.095	0.590
	1.047	1.519	3.662	0.832	0.890	0.571
	1.179	1.785	3.929	0.628	0.835	0.627
Average	1.15	1.62	3.63	0.77	0.94	0.60
32	1.170	2.169	4.403	1.240	1.371	1.026
	1.173	2.193	4.433	1.297	1.335	0.980
	0.979	2.167	4.122	1.296	1.394	0.894
Average	1.11	2.18	4.32	1.28	1.37	0.97
50	0.921	2.563	5.552	2.300	1.787	1.108
	1.586	2.621	5.094	1.654	1.794	1.179
	1.516	2.514	5.493	1.904	1.589	1.204
Average	1.34	2.57	5.38	1.95	1.72	1.16
75	1.258	3.353	5.673	2.777	3.380	2.360
	1.112	3.212	6.209	3.729	2.843	2.425
	1.457	3.325	6.795	2.709	2.854	2.478
Average	1.28	3.30	6.23	3.07	3.03	2.42
83	1.468	3.936	7.672	5.519	3.480	3.047
	1.416	3.871	6.714	4.366	3.504	3.075
	1.648	4.343	7.227	3.500	3.353	3.420
Average	1.51	4.05	7.20	4.46	3.45	3.18
97	1.603	7.298	11.854	4.978	5.181	5.329
	1.459	6.848	12.109	5.393	5.165	5.262
	1.349	7.077	12.132	5.964	5.364	5.204
Average	1.47	7.07	12.03	5.45	5.24	5.27

Analysis of the values of the R coefficients placed in Table 7 proves that the solutions were not found for all the 24 adopted models. In such instances, dashes are placed in the table above. Amongst all the analyzed equations, the highest compatibility between the mathematical models and the experimental data for the six materials in question was observed in the equations of Chen and Chen Jovanovič's—for multi-layer adsorption, and Hüttig's. For those models, the highest values of the R correlation coefficient were obtained. Further, some satisfactory results were recorded, using the Dubinin–Serpiński's and D'Arcy–Watt's models; not in all cases, however, solutions were found. For the ceramic brick, the equation of Chen and Chen describes the isotherms satisfactorily for 5 °C, 20 °C and 35 °C. At 20 °C, the D'Arcy–Watt's equation is better; however, it does not provide solution for the above mentioned two temperature levels. Nevertheless, the situation with the silicate brick seems to be quite different, as in this case there are several functions, which yield quite good descriptions of the experimental data for all the temperature levels. These equations include: the Chen and Chena, the Jovanovič's—for multi-layer adsorption, the Dubinin–Serpinski's and the Hüttig's. However, from among them, the highest accuracy is provided by the Chen and Chen models. It is non-disputably the best model also in case of the cellular concrete.

Amongst all the analysed equations, the highest compatibility between the mathematical models and the experimental data for the three mortars was observed also in the equations of Chen and Chen. With this model, the highest values of the R coefficient were recorded in the most of temperatures.

3 Conclusions

Obtained in non-stationary tests of sorption processes, the equilibrium sorption moisture values for the six materials, all collected at the three temperature and six humidity levels, were used to draw sorption isotherms. Then the isotherms were confronted with the isotherms under the Brunauer's and IUPAC classifications. The obtained isotherms represent by their nature type II isotherm, according to the classification mentioned before. This isotherm type relates to appearance of a multi-molecular adsorption film during physical adsorption. On those curves, it is possible to identify three sections respective to three stages of gas adsorption on a solid body. The first section is typical of

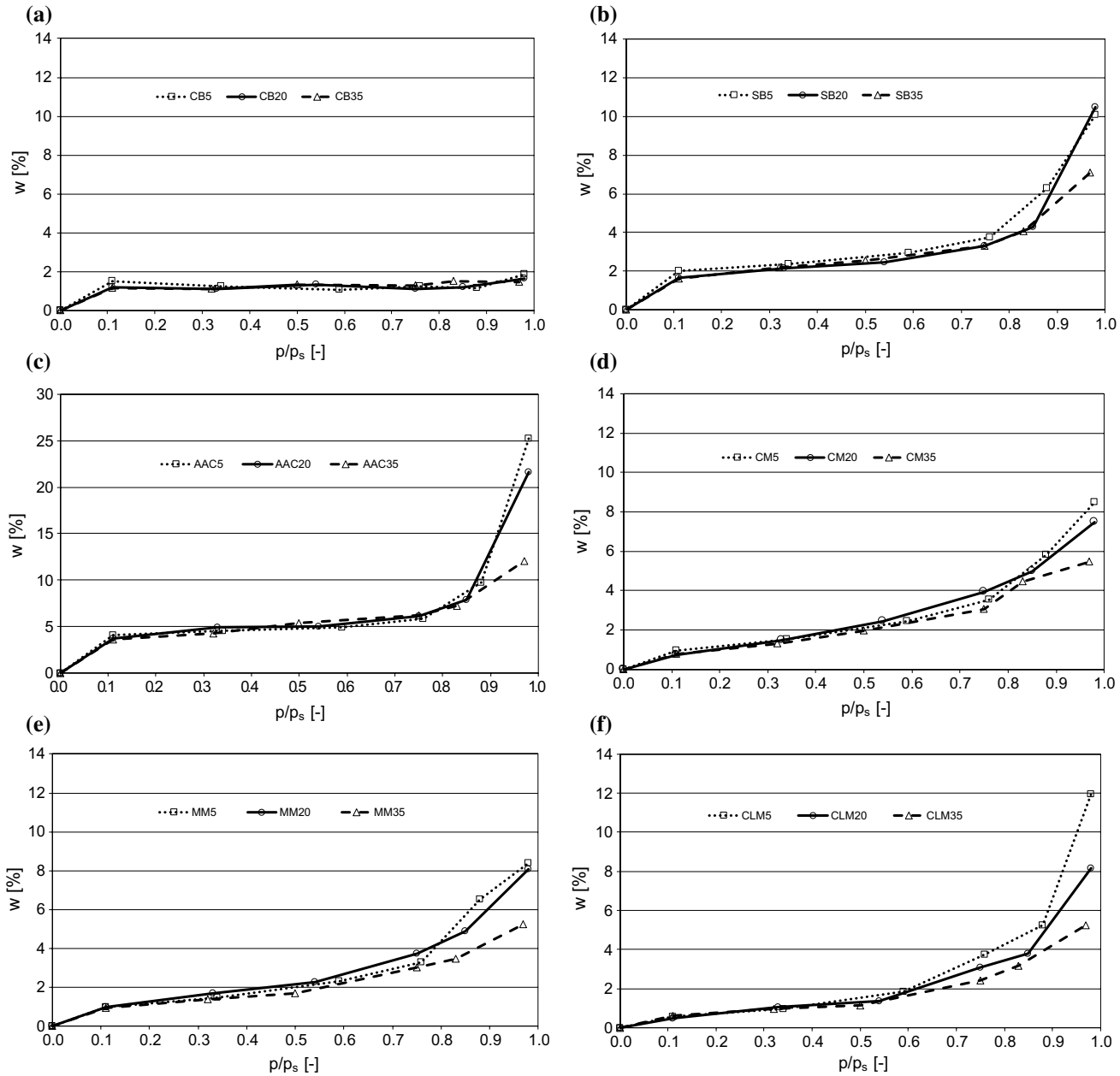

Fig. 4 Sorption isotherms at 5, 20, 35 °C for: **a** ceramic brick CB, **b** silicate brick SB, **c** autoclaved aerated concrete AAC, **d** cement mortar CM, **e** modified mortar MM, **f** cement–lime mortar CLM

isotherm type I, where, at low relative humidities, a monomolecular film of the adsorbed substance gets formed on the surface of the adsorbent. Further on, along with the increasing relative humidity, formation of a multi-molecular film takes place. Above the humidity of ca. 80 %, the process of capillary condensation in the adsorbent mezzopores begins. Obtained results of the research manifest the influence of the structural construction of materials to the quantity of the sorption humidity. Because a big specific surface, porousness and sizes of pores are one of the factors affecting the sorption ability of porous bodies.

The authors undertook to test whether exists a possibility to describe very different courses of the sorption isotherms by means of one universal formula. In order to describe the experimentally obtained sorption isotherms for the porous building materials in study, the functions listed in Table 6 were used. The analysis results, reflecting the suitability of the individual models applied, are presented in Table 7.

Having analysed all the data, it is declared that the Chen's equation reflects relation $w = f(\varphi)$ the best. For this model, a high accordance between the experimental and the theoretical courses was achieved for all the tested materials,

Table 6 Tested isotherm equations

No.	Authors	Equations
1	Henry	$a = K_{a,p}p$
2	Langmuir	$a = \frac{a_m kp}{1+kp}$
3	Freundlich	$a = kp^{\frac{1}{n}}$
4	Spis	$a = a_m \frac{(kp)^{1/n}}{1+(kp)^{1/n}}$
5	Dubinin and Raduszkiewicz	$a = a_0 e^{-b\left(RT\ln\frac{p_s}{p}\right)^2} = a_0 10^{-D\left(\log\frac{p_s}{p}\right)^2}$
6	Redlich–Peterson	$a = \frac{Ap}{1+Bp^n}$
7	Kisarow	$a = \frac{AB\left(\frac{p}{p_s}\right)^n}{1+B\left(\frac{p}{p_s}\right)^n}$
8	BET	$a = \frac{a_m C\frac{p}{p_s}}{\left(1-\frac{p}{p_s}\right)\left[1+(C-1)\frac{p}{p_s}\right]}$
9	Harkins–Jury	$\log\frac{p}{p_s} = B - \frac{A}{\upsilon^2}$
10	Hüttig	$a = \frac{a_m C\frac{p}{p_s}\left(1+\frac{p}{p_s}\right)}{1+C\frac{p}{p_s}}$
11	Łykow	$u_L = u_{hig}\left(1-\frac{\ln\varphi}{d}\right)^{-1}$
12	Hansen	$u_L = u_{hig}\left(1-\frac{\ln\varphi}{A}\right)^{-\frac{1}{n}}$
13	Chen and Chen	$u_L = \frac{a\varphi}{(1+b\varphi)(1-c\varphi)}$
14	Kisielew	$h = \frac{\Theta'}{K_1'(1-\Theta')\left(1+K_n\Theta'\right)}$
15	Hill and de Boer	$h = \frac{\Theta}{K_1(1-\Theta)}\exp\left(\frac{\Theta}{1-\Theta} - K_2\Theta\right)$
16	Jovanovič for single-layer adsorption	$a = a_m\left[1-\exp\left(-a''h\right)\right]$
17	Jovanovič for multi-layer adsorption	$a = a_m\left[1-\exp\left(-a''h\right)\right]\exp\left(b''h\right)$
18	Dubinin	$a = \frac{a_0 k\frac{p}{p_s}}{1-\frac{p}{p_s}}$
19	Dubinin–Serpinski	$\frac{p}{p_s} = \frac{a}{k(a_0+a)\left(1-\frac{k-1}{k}\frac{a}{a_s}\right)}$
20	D'Arcy–Watt	$a = \frac{K_1K_2\frac{p}{p_s}}{1-K_1\frac{p}{p_s}} + C\frac{p}{p_s} + \frac{k_1k_2\frac{p}{p_s}}{1-k_1\frac{p}{p_s}}$
21	Dubinin–Astachow	$a = \rho_c W_0 \exp\left[-\left(\frac{RT\ln\frac{p}{p_s}}{E}\right)^n\right]$
22	Toth	$a = a_m\frac{kp}{\left[1+(kp)^t\right]^{1/t}}$
23	Unilan	$a = \frac{a_m}{2s}\ln\left(\frac{1+kpe^s}{1+kpe^{-s}}\right)$
24	Keller	$a = a_m\alpha_m\frac{kp}{\left[1+(kp)^\alpha\right]^{1/\alpha}}$

at all the three temperature levels. In case of Chen's model the coefficient of correlation R for particular materials were included in the intervals: CB 0.89–0.99; SB $\approx$ 0.99; AAC 0.98–0.99; CM 0.99–1.0; MM 0.99–1.0; CLM $\approx$ 1.0. Basing on the compiled results stated in Table 7, the authors may state that the Chen's equation approximates all experimental data in a satisfactory manner and can be used successfully to describe sorption isotherms for such building materials as ceramic brick, silicate brick, autoclaved aerated concrete or cement mortars of the different kinds.

Table 7 Results of estimation of *R* parameters for the sorption isotherm equations

Material	Authors	T = 5 °C	T = 20 °C	T = 35 °C
Ceramic brick CB	Langmuir	0.8868	0.9327	0.9576
	Hüttig	0.8150	0.9020	0.9634
	Chen and Chen	**0.8916**	0.9501	**0.9899**
	Jovanovič—single-layer	0.8868	0.9341	0.9684
	Jovanovič—multi-layer	0.8908	0.9490	0.9899
	Dubinin–Serpinski	0.7812	0.7795	0.8907
	D'Arcy–Watt	–	**0.9702**	–
	Toth	0.8868	0.9414	0.9852
	Unilan	0.8868	0.9327	0.9576
	Keller	0.8868	0.9408	–
Silicate brick SB	Henry	0.8798	0.8209	0.9123
	BET	0.6046	0.8077	0.4760
	Hüttig	0.9125	0.8629	0.9187
	Chen and Chen	**0.9958**	**0.9923**	**0.9935**
	Jovanovič—single-layer	0.8798	0.8209	0.9123
	Jovanovič—multi-layer	0.9626	0.9417	0.9631
	Dubinin	0.5264	0.7639	0.2520
	Dubinin–Serpinski	0.9171	0.9171	0.9215
	D'Arcy–Watt	0.9758	0.9869	–
	Unilan	0.5223	0.4574	0.5905
Autoclaved aerated concrete AAC	Henry	0.7542	0.7847	0.8997
	Langmuir	0.4178	0.4527	0.6642
	Spis	–	0.4527	0.6642
	BET	0.8912	0.8295	–
	Hüttig	0.8027	0.8258	0.9091
	Chen and Chen	**0.9876**	**0.9825**	**0.9858**
	Jovanovič—single-layer	0.7542	0.7847	0.8998
	Jovanovič—multi-layer	0.9338	0.9167	0.9592
	Dubinin	0.8613	0.7881	–
	Unilan	0.4178	0.4527	0.6642
Cement mortar CM	Henry	0.9120	0.9551	0.9710
	Langmuir	0.4780	0.5039	0.5367
	BET	0.6332	0.4621	0.3392
	Hüttig	0.9511	0.9831	0.9869
	Chen and Chen	**0.9980**	**0.9997**	0.9916
	Jovanovič—single-layer	0.9120	0.9550	0.9710
	Jovanovič—multi-layer	0.9927	0.9987	**0.9941**
	Dubinin–Serpinski	0.9704	0.9873	0.9836
	D'Arcy–Watt	0.9947	0.9990	0.9903
	Unilan	0.4780	0.5039	0.5367
Modified mortar MM	Henry	0.9039	0.9252	0.9609
	Langmuir	0.4692	0.4973	0.5602
	Kisarow	–	–	0.9697
	BET	0.5895	0.5894	0.4364
	Hüttig	0.9451	0.9584	0.9752
	Chen and Chen	0.9875	**0.9997**	**0.9988**
	Jovanovič—single-layer	0.9039	0.9252	0.9609
	Jovanovič—multi-layer	**0.9887**	0.9908	0.9954
	Dubinin–Serpinski	0.9653	0.9673	0.9674
	D'Arcy–Watt	0.9861	0.9953	0.9910

Table 7 continued

Material	Authors	T = 5 °C	T = 20 °C	T = 35 °C
Cement–lime mortar CLM	Henry	0.8095	0.8571	0.9196
	Kisarow	0.9775	**0.6546**	–
	BET	0.9015	0.8317	0.7338
	Hüttig	0.8660	0.9089	0.9580
	Chen and Chen	0.9983	**0.9981**	**0.9977**
	Jovanovič—single-layer	0.8095	0.8571	0.9196
	Jovanovič—multi-layer	0.9852	0.9886	0.9947
	Dubinin	0.8801	0.8000	0.6622
	Dubinin–Serpinski	0.9861	0.9777	0.9714
	D'Arcy–Watt	**0.9988**	0.9978	0.9951

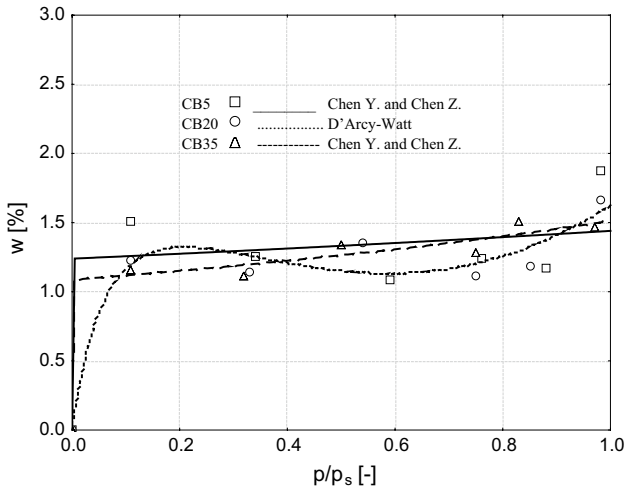

Fig. 5 The best results of estimation of sorption isotherms for CB at each of the temperature levels: **a** 5 °C: Chen and Chen, **b** 20 °C: D'Arcy–Watt, **c** 35 °C: Chen and Chen

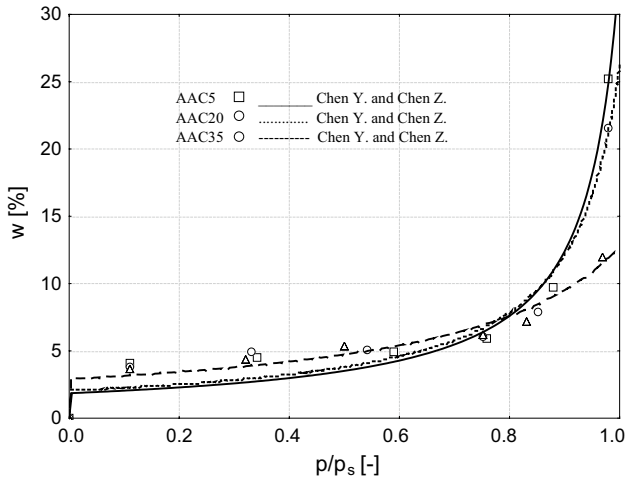

Fig. 7 The best results of estimation of sorption isotherms for AAC at each of the temperature levels: **a** 5 °C: Chen and Chen, **b** 20 °C: Chen and Chen, **c** 35 °C: Chen and Chen

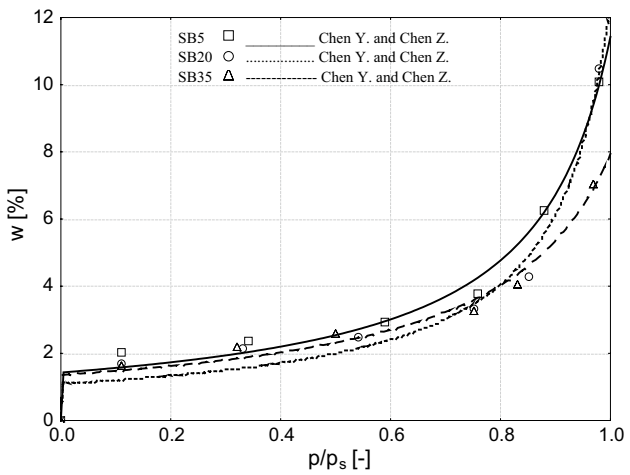

Fig. 6 The best results of estimation of sorption isotherms for SB at each of the temperature levels: **a** 5 °C: Chen and Chen, **b** 20 °C: Chen and Chen, **c** 35 °C: Chen and Chen

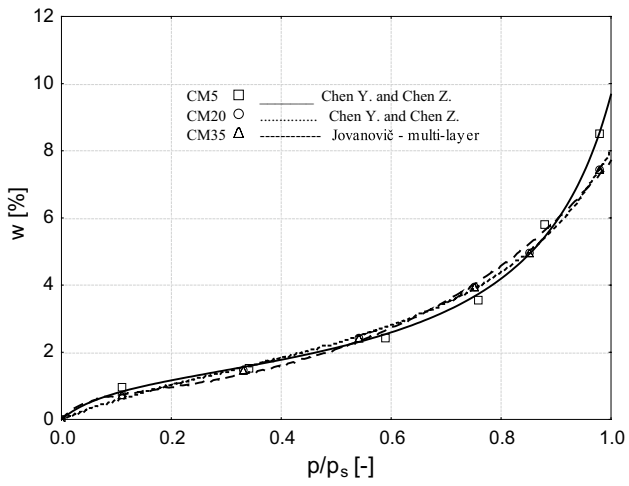

Fig. 8 The best results of estimation of sorption isotherms for CM at each of the temperature levels: **a** 5 °C: Chen and Chen, **b** 20 °C: Chen and Chen, **c** 35 °C: Jovanovič—multi-layer

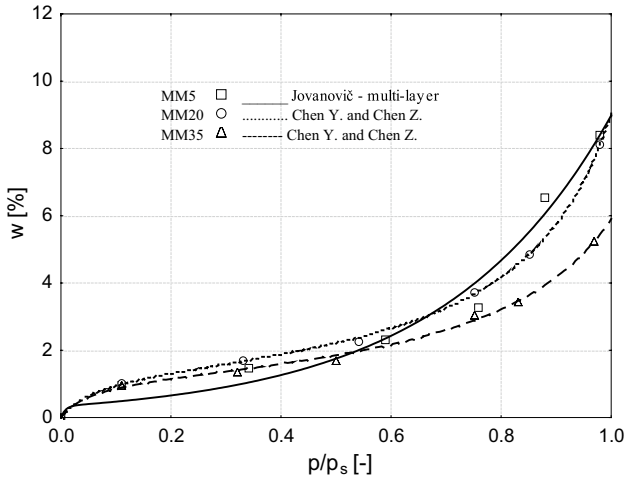

Fig. 9 The best results of estimation of sorption isotherms for MM at each of the temperature levels: **a** 5 °C: Jovanovič—multi-layer, **b** 20 °C: Chen and Chen, **c** 35 °C: Chen and Chen

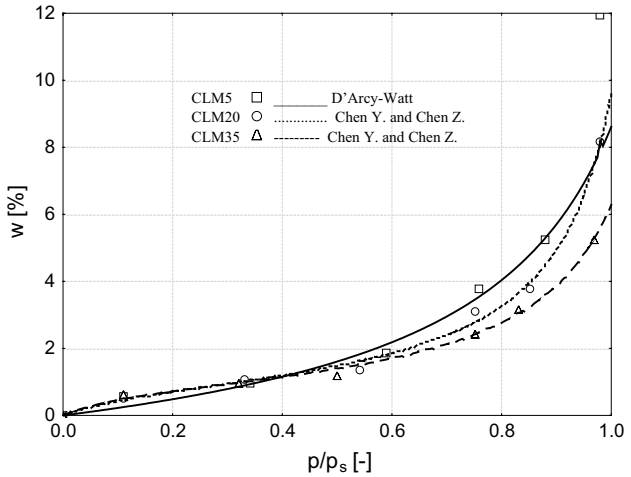

Fig. 10 The best results of estimation of sorption isotherms for CLM at each of the temperature levels: **a** 5 °C: D'Arcy–Watt, **b** 20 °C: Chen and Chen, **c** 35 °C: Chen and Chen

Under planning is applying of the microstructural parameters typical for every material to describe their sorption isotherms.

Acknowledgments The measurements analysed in this study are a part of the research project funded by the Ministry of Education and Science of Poland (Grant Number 4 T07E 033 30).

Compliance with ethical standards

Conflict of interest The authors declare that there is no conflict of interest.

References

1. Jenisch R (1996) Tauwasserschäden. IRB, Stuttgart
2. Rahn A, Bonk M (2008) Analyse von Feuchte- und Salzschäden an historischen Gebäuden. Bauphysik-Kalender, Verlag Ernst & Sohn, Berlin, pp 469–486
3. Unčik S, Struharova A, Hlavinkova M (2013) Effect of bulk density and moisture content on the properties of autoclaved aerated concrete. Cem Lime Concr 4:189–196
4. Garbalińska H, Wygocka A (2014) Microstructure modification of cement mortars: effect on capillarity and frost-resistance. Constr Build Mater 51:258–266
5. Wygocka A (2010) Capillarity of cement mortars modified with polypropylene fibers. PhD thesis, West Pomeranian University of Technology (in Polish)
6. Siwińska A (2008) Relation between sorption isotherm and thermal conductivity coefficient of porous material. PhD thesis, West Pomeranian University of Technology (in Polish)
7. Siwińska A, Garbalińska H (2011) Thermal conductivity coefficient of cement-based mortars as air relative humidity function. Heat Mass Transf 47(9):1077–1087
8. PN-EN ISO 12571:2002 (2002) Hygrothermal performance of building materials and products—determination of hygroscopic sorption properties
9. Plagge R, Funk M, Scheffler G (2006) Experimentelle Bestimmung der hygrischen Sorptionsisotherme und des Feuchtetransportes unter instationären Bedingungen. Bauphysik 28(2):81–87
10. Plagge R, Grunewald J, Häupl P (1999) Simultane Bestimmung der hygrischen Sorptionsisotherme und der Wasserdampfpermeabilität. In: Feuchtetag'99, Umwelt, Meβverfahren, Anwendungen DGZfP-Berichtsband BB 69-CD Poster 22
11. Plagge R, Scheffler G, Grunewald J (2006) Measurement of water retention and moisture conductivity at transient conditions. In: Proc. monogr. eng. wate., Concordia University, Montreal. Taylor & Francis Group, London, pp 129–136
12. Scheffler G, Plagge R, Grunewald J (2006) Evaluation of instantaneous profile measurements indicating dependencies of moisture transport on hysteresis and dynamics. In: Proc. monogr. eng. wate., Concordia University, Montreal. Taylor & Francis Group, London, pp 121–128
13. Markova N, Sparr E, Wadsö L (2001) On application of an isothermal sorption microcalorimeter. Thermochim Acta 374:93–104
14. Wadsö I, Wadsö L (1996) A new method for determination of vapour sorption isotherms using a twin double microcalorimeter. Thermochim Acta 271:179–187
15. McGregor F, Heath A, Fodde E (2014) Conditions affecting the moisture buffering measurement performed on compressed earth blocks. Build Environ 75:11–18
16. McGregor F, Heath A, Shea A (2014) The moisture buffering capacity of unfired clay masonry. Build Environ 82:599–607
17. Wu M, Johannesson B, Geiker M (2014) A study of the water vapor sorption isotherms of hardened cement pastes: possible pore structure changes at low relative humidity and the impact of temperature on isotherms. Cem Concr Res 56:97–105

18. Anderberg A, Wadsö L (2008) Method for simultaneous determination of sorption isotherms and diffusivity of cement-based materials. Cem Concr Res 38(1):89–94
19. Espinosa RM, Franke L (2006) Influence of the age and drying process on pore structure and sorption isotherms of hardened cement paste. Cem Concr Res 36:1969–1984
20. Janz M (1997) Moisture transport and fixation in porous materials at high moisture levels. PhD thesis, Lund Institute of Technology, Lund University
21. Johannesson BF (2002) Prestudy on diffusion and transient condensation of water vapor in cement mortar. Cem Concr Res 3:955–962
22. Garbalińska H, Kowalski SJ, Staszak M (2012) Evaluation of moisture diffusion coefficients in cement plasters based on desorption processes. In: 18th international drying symposium: conference proceedings. Department of Chemical and Biochemical Engineering, College of Chemistry and Chemical Engineering, Xiamen University, Xiamen
23. Tada S, Watanabe K (2005) Dynamic determination of sorption isotherm of cement based materials. Cem Concr Res 35(12):2271–2277
24. Jerman M, Keppert M, Vyborny J (2013) Hygric, thermal and durability properties of autoclaved aerated concrete. Constr Build Mater 41:352–359
25. Koronthalyova O (2011) Moisture storage capacity and microstructure of ceramic brick and autoclaved aerated concrete. Constr Build Mater 25:879–885
26. Jiŕičková M, Černý R (2002) Hygric and thermal properties of capillary active rock wool thermal insulation. In: Building physics 2002—6th nordic symposium, pp 461–468
27. Valovirta I, Vinha J (2002) Hemp as insulation material in wooden houses. In: Building physics 2002—6th nordic symposium, pp 469–475
28. Kumaran MK (2006) A thermal and moisture property database for common building and insulation materials. NRCC-45692 ASHRE Trans 112(2):1–24
29. Poděbradská J, Toman J, Drchalová J (2002) Hygric and thermal properties of glass-fiber reinforced cement composites. In: Building physics 2002—6th nordic symposium, pp 477–484
30. Keller J, Staudt R (2005) Gas adsorption equilibria. Experimental methods and adsorption isotherms. Springer, New York
31. Chen Y, Chen Z (1998) Transfer function method to calculate moisture absorption and desorption in buildings. Build Environ 33(4):201–207
32. Kumar KV (2007) Optimum sorption isotherm by linear and non-linear methods for malachite green onto lemon peel. Dyes Pigments 74:595–597
33. Kumar KV, Sivanesan S (2005) Comparison of linear and non-linear method in estimating the sorption isotherm parameters for safranin onto activated carbon. J Hazard Mater B123:288–292
34. Kumar KV, Sivanesan S (2005) Prediction of optimum sorption isotherm: Comparison of linear and non-linear method. J Hazard Mater B126:198–201
35. Lowell S, Shields JE, Thomas MA (2004) Characterization of porous solids and powders: surface area, pore size and density. Kluwer Academic Publishers, Dordrecht
36. Lagorosse S, Campo MC, Magalhães FD (2005) Water adsorption on carbon molecular sieve membranes: experimental data and isotherm model. Carbon 43:2769–2779
37. Osanyintola OF, Simonson CJ (2006) Moisture buffering capacity of hygroscopic building materials: experimental facilities and energy impact. Energy Build 38:1270–1282
38. Perry RH, Green DW (1997) Perry's chemical engineers' handbook. McGraw-Hill, New York
39. Rouquerol J, Rouquerol F, Sing K (1998) Absorption by powders and porous solids. Academic, New York
40. Yuh-Shan H (2004) Selection of optimum sorption isotherm. Carbon 42:2115–2116
41. Pavlík Z, Žumár J, Medved I, Černý R (2012) Water vapor adsorption in porous building materials: experimental measurement and theoretical analysis. Transp Porous Med 95:21–23
42. Furmaniak S (2012) The alternative model of water vapour sorption in porous building materials. Transp Porous Med 91:939–954
43. Brunauer S, Deming LS, Deming WE (1940) On a theory of the van der Waals adsorption of gases. J Am Chem Soc 62:1723–1732
44. Chen H-Y, Chiachung C (2014) Equilibrium relative humidity method used to determine the sorption isotherm of autoclaved aerated concrete. Build Environ. doi:10.1016/j.buildenv.2014.07.021
45. Feng C, Janssen H, Wu C, Feng Y, Meng Q (2013) Validating various measures to accelerate the static gravimetric sorption isotherm determination. Build Environ 69:64–71